USP10 Promotes Fibronectin Recycling, Secretion, and Organization

Andrew T. Phillips,[1] Edward F. Boumil,[1] Nileyma Castro,[1,2] Arunkumar Venkatesan,[1] Eugenio Gallo,[3] Jarrett J. Adams,[3] Sachdev S. Sidhu,[3] and Audrey M. Bernstein[1,2]

[1]Department of Ophthalmology and Visual Sciences, SUNY Upstate Medical University, Syracuse, New York, United States
[2]Syracuse VA Medical Center, New York VA Health Care, Syracuse, New York, United States
[3]Department of Molecular Genetics, University of Toronto, Toronto, Ontario, Canada

Correspondence: Audrey M. Bernstein, Department of Ophthalmology and Visual Sciences, SUNY Upstate Medical University, 750 East Adams Street, Syracuse, NY 13210, USA;
bernstea@upstate.edu.

Received: July 13, 2021
Accepted: September 27, 2021
Published: October 19, 2021

Citation: Phillips AT, Boumil EF, Castro N, et al. USP10 promotes fibronectin recycling, secretion, and organization. *Invest Ophthalmol Vis Sci.* 2021;62(13):15.
https://doi.org/10.1167/iovs.62.13.15

Purpose. Integrins play a central role in myofibroblast pathological adhesion, overcontraction, and TGFβ activation. Previously, we demonstrated that after corneal wounding, αv integrins are protected from intracellular degradation by upregulation of the deubiquitinase USP10, leading to cell-surface integrin accumulation. Because integrins bind to and internalize extracellular matrix (ECM), we tested whether extracellular fibronectin (FN) accumulation can result from an increase in integrin and matrix recycling in primary human corneal fibroblasts (HCFs).

Methods. Primary HCFs were isolated from cadaver eyes. HCFs were transfected with either USP10 cDNA or control cDNA by nucleofection. Internalized FN was quantified with a FN ELISA. Recycled extracellular integrin and FN were detected with streptavidin-488 by live cell confocal microscopy (Zeiss LSM 780). Endogenous FN extra domain A was detected by immunocytochemistry. Cell size and removal of FN from the cell surface was determined by flow cytometry.

Results. USP10 overexpression increased $\alpha5\beta1$ (1.9-fold; $P < 0.001$) and αv (1.7-fold; $P < 0.05$) integrin recycling, with a concomitant increase in biotinylated FN internalization (2.1-fold; $P < 0.05$) and recycling over 4 days (1.7–2.2-fold; $P < 0.05$). The dependence of FN recycling on integrins was demonstrated by $\alpha5\beta1$ and αv integrin blocking antibodies, which, compared with control IgG, decreased biotinylated FN recycling (62% and 84%, respectively; $P < 0.05$). Overall, we established that extracellular FN was composed of approximately 1/3 recycled biotinylated FN and 2/3 endogenously secreted FN.

Conclusions. Our data suggest that reduced integrin degradation with a subsequent increase in integrin/FN recycling after wounding may be a newly identified mechanism for the characteristic accumulation of ECM in corneal scar tissue.

keywords: myofibroblast, integrin, fibrosis, scarring, wound healing, cornea, deubiquitinase, fibronectin

Scarring in the eye can result in visual disability or blindness. In particular, because the cornea is transparent, a scar severely impacts vision.[1] For scientific discovery of scarring mechanisms, the cornea is a very useful model for studying wound healing, as scarring can be easily evaluated.[2,3] Corneal stromal wounding induces an influx of myofibroblasts and immune cells into the cornea.[4,5] The persistence of pathological myofibroblasts and fibrotic matrix forms a scar, blocking transmission of light.[6,7] Integrin-mediated adhesion promotes myofibroblast differentiation by increasing cell adhesion and cellular tension, required for the assembly of alpha-smooth muscle actin (α-SMA) stress fibers characteristic of myofibroblasts.[6,8] Integrins also activate latent, matrix-associated endogenous TGFβ by binding to the arginine–glycine–aspartic acid (RGD) domain in its latency-associated peptide.[9–11] FN-binding integrins (αv and $\alpha5\beta1$) in particular are strongly associated with fibrotic outcomes.[9,12–18]

Our previous work discovered that the deubiquitinase (DUB) USP10 gene and protein expression were increased in human corneal myofibroblasts.[13] DUBs remove ubiquitin from proteins, preventing degradation. We found that USP10 is a DUB for integrin subunits $\beta1$ and $\beta5$ but not on $\beta3$.[13] (The αv integrin subunit is not directly ubiquitinated but is degraded with the β subunit).[19,20] Correspondingly, knockdown of USP10 gene expression increased ubiquitination of integrin $\beta1$ and $\beta5$ subunits, leading to decreased αv/$\beta1$/$\beta5$ protein levels, whereas gain of USP10 expression increased these protein levels without altering integrin gene expression.[13] As a result of cell-surface integrin accumulation, TGFβ is activated, leading to increased gene expression and organization of the fibrotic markers, α-SMA and fibronectin extra domain A (FN-EDA).[13] Blocking either TGFβ signaling or cell-surface αv integrins after USP10 overexpression prevented or reduced these fibrotic markers, respectively.[13] Furthermore, knockdown of USP10 with USP10-targeting

siRNA after wounding in an ex vivo pig cornea organ culture model and in an in vivo rabbit corneal model significantly reduced the induction of fibrotic markers and promoted regenerative healing[13,21,22] These data suggest that controlling integrin levels via DUB expression is a novel method to control scarring and fibrosis.

Here, we have continued this work by testing if the USP10-mediated increase in integrins on the cell surface after wounding is an undiscovered mechanism for increasing extracellular matrix, a hallmark of scarring and fibrosis. We have focused this study on $\alpha5\beta1$ and αv integrins and the matrix molecule, fibronectin. In a stepwise manner, FN secreted by cells is organized to assemble into fibrils (fibrillogenesis).[23] As assembly progresses, short detergent-soluble fibrils are converted into a dense detergent-insoluble fibrillar network.[24] The FN extracellular matrix is a dynamic scaffold that is a central player in cell repair, adhesion, migration, and invasion. The αv integrins, along with the classical FN receptor $\alpha5\beta1$ integrin, bind to and coordinate the organization and endocytosis of FN through the binding of FN RGD domains.[25] Using single-cell force microscopy, it was demonstrated that αv integrins bind first to FN, signaling to $\alpha5\beta1$ to form additional adhesion sites. This crosstalk strengthens adhesions to FN.[26] Integrins also mediate the endocytosis of FN,[27] but large organized FN fibrils cannot be endocytosed. Membrane-type 1 matrix metalloproteinase (MT1-MMP), a membrane-bound MMP, plays a key role in the extracellular FN cleavage that is necessary for FN endocytosis and subsequent intracellular degradation[28,29] or recycling back to the cell surface.[30,31]

Disrupted FN homeostasis leading to a buildup of extracellular FN and, specifically, the fibrotic cellular splice variant, FN-EDA, is linked to the activation of TGFβ and a wide range of disease pathologies, including cardiac, liver, kidney, and dermal fibrosis, as well as glaucoma.[32–38] Here, we demonstrate that overexpression of the DUB USP10 increases $\alpha5\beta1$ and αv integrin recycling to the cell surface. This increase in integrin recycling also promotes endocytosis and subsequent recycling of FN. Together, these data demonstrate that integrin ubiquitination status affects not only the recycling of integrin to the cell surface but also the recycling of integrin-bound matrix.

Materials and Methods

Antibodies and Reagents

Flag-HA-USP10 (plasmid 22543) for transient overexpression was obtained from Addgene (Watertown, MA, USA). Antibody against $\alpha5\beta1$ (volociximab; 2-52680) was obtained from Novus Biologicals (Littleton, CO, USA),[71,72] and the antibody against αv (AV-1b/2b) was produced in the lab of Dr. Sachdev S. Sidhu at the University of Toronto, Ontario Canada.[73] Fibronectin fluorescein isothiocyanate (FITC; F2733) was obtained from Sigma-Aldrich (St. Louis, MO, USA). Herring sperm DNA (Invitrogen 15634-017) was obtained from Thermo Fisher Scientific (Waltham, MA, USA). Secondary anti-rabbit-488 conjugated antibody (111-545-003) was obtained from The Jackson Laboratory (Bar Harbor, ME, USA). Biotinylated FN (FNR03) was obtained from Cytoskeleton, Inc. (Denver, CO, USA). HRP-conjugated streptavidin (405210) was obtained from BioLegend (San Diego, CA, USA). Alexa Fluor 488-conjugated anti-fibronectin antibody (IST-9, sc-59826) was obtained from Santa Cruz Biotechnology (Santa Cruz, CA, USA).

Cell Culture

Human cadaver corneas from unidentifiable diseased subjects were obtained from the Syracuse Eye Bank (Syracuse, NY, USA) and The Eye-Bank for Sight Restoration (New York, NY, USA). The SUNY Upstate Medical University Institutional Review Board informed us that, as described under Title 45 CFR Part 46 of the Code of Federal Regulations, unidentifiable cadaver tissue does not constitute research in human subjects. Hence, the experiments performed in this report do not require their approval or waiver. However, all tissue was screened for pathogens as if it were to be transplanted for clinical use in humans. We obtained tissue after the screening process. HCFs were isolated as described previously[74] and maintained in complete media: Invitrogen Dulbecco's Modified Eagle Medium (DMEM)/Nutrient Mixture F-12 with 10% fetal bovine serum (FBS; Atlanta Biologicals, Flowery Branch, GA, USA) with Invitrogen ABAM (antibiotic antimycotic) and gentamicin. For experiments, except where noted, cells were plated on 10-µg/mL bovine collagen (Purcol; Advanced BioMatrix, Carlsbad, CA, USA) in supplemented serum-free media (SSFM), comprised of DMEM/F-12 plus RPMI 1640 Vitamin Mix (Sigma-Aldrich); ITS Liquid Media Supplement (Sigma-Aldrich); 1-mg/mL glutathione (Sigma-Aldrich); 2-mM L-glutamine, 1-mM sodium pyruvate, and 0.1-mM non-essential amino acids (Invitrogen); and ABAM and gentamicin (Sigma-Aldrich).

Live Cell Integrin Recycling Assay

HCFs (P3 Primary Cell Solution; Lonza Group, Basel, Switzerland) were transfected with 2 µg of control or 2 µg USP10 cDNA and replated in DMEM/F-12 and 1% FBS. Forty-eight hours after transfection, the cells were blocked with Herring Sperm DNA (10 µg/mL) for 30 minutes. Cells were treated with antibody against $\alpha5\beta1$ and αv at 10 µg/mL for 30 minutes. Cells were then stripped (0.2-M acetic acid, 0.5-M NaCl) for 30 seconds and incubated for 90 minutes prior to washing and incubation with Alexa Fluor 488 anti-rabbit antibody for 30 minutes. Live cells were imaged on a LSM 780 confocal microscope (Carl Zeiss, Jena, Germany) and analyzed using the Analyze Particles plugin for ImageJ (National Institutes of Health, Bethesda, MD, USA).

Biotinylated FN ELISA

HCFs were transfected (P3 Primary Cell Solution) with 2 µg of control or 2 µg USP10 cDNA and replated in DMEM/F-12 and 1% FBS. Forty-eight hours after transfection, the cells were loaded with 10 µg biotinylated FN for 3 hours. The cells were passaged with trypsin and resuspended in 100 µL of a lysis buffer (50-mM Tris HCl, pH 8.8; 150-mM NaCl; 0.5% Triton X-100) containing protease inhibitor tablets (Roche, Basel, Switzerland) and PMSF (Thermo Fisher Scientific). After centrifugation of the lysates, the supernatant was collected and the pellet was resuspended in 100 µL of the same lysis buffer. After thorough vortexing, the lysates were added together and centrifuged again, and the supernatant was collected. The protocol for the Quantikine ELISA kit (DFBN10; R&D Systems, Minneapolis, MN, USA) was followed. The lysates were diluted in R&D Systems proprietary diluent in a 1:4 ratio. However, the ELISA was modified by using a 1:100 HRP-conjugated streptavidin to detect only biotinylated FN. Signal was detected with an Epoch spectrophotometer (BioTek, Winooski, VT, USA), and samples were analyzed against a standard curve.

Investigative Ophthalmology & Visual Science

Fixed Cell FN-FITC Recycling Assay

HCFs were plated on glass coverslips and treated with FN-FITC (F2733; Sigma-Aldrich) for 3 hours in DMEM/F-12 and 1% FBS. One group was fixed with 3% paraformaldehyde (Thermo Fisher Scientific) in PBS and imaged. The remaining cells were passaged with trypsin; replated; fixed in 3% paraformaldehyde; and imaged at 2, 18, 26, and 72 hours after passage on an ECLIPSE Ni microscope (Nikon, Tokyo, Japan) (Fig. 2A).

Flow Cytometry

HCFs (200,000) were plated in DMEM/F-12 and 1% FBS. The next day, cells were treated with 4 µg/mL of FN-FITC for 3 hours. The cells were then washed with Gibco PBS (Thermo Fisher Scientific), detached with trypsin (Corning, Manassas, VA, USA) and collected in DMEM/F-12 with 1% FBS. The cells were counted and centrifuged at 100*g* for 5 minutes, washed with PBS, and pelleted again. The cell pellet was resuspended in PBS plus 1% BSA with and without 2 mg/mL of Trypan Blue and analyzed by flow cytometry (BD LSRFortessa; BD Biosciences, Franklin Lakes, NJ, USA). Data analysis was performed in FlowJo 10.7.2 (Fig. 2B).

HCFs (1,000,000) were transfected with 2 mg control FLAG and USP10 FLAG cDNA (Sigma-Aldrich). After 48 hours, cells were detached with TrypLE Express (12605028; Thermo Fisher Scientific), washed at 3000 rpm for 2 minutes, and resuspended in FACS buffer. The cells were stained with live/dead stain (LIVE/DEAD Fixable Violet Dead Cell Stain Kit, L34963; Thermo Fisher Scientific) and fixed with 3% paraformaldehyde. Next, the cells were permeabilized with 0.2% saponin containing FACS buffer and stained with anti-FLAG antibody (9A3, 8146S; Cell Signaling Technology, Danvers, MA, USA), followed by Alexa Fluor 647 AffiniPure Goat Anti-Mouse IgG (H+L) (115-605-003; Jackson ImmunoResearch, West Grove, PA, USA). The cells were then washed and resuspended in FACS buffer and analyzed using a BD LSR II flow cytometer. Data analysis was performed in FlowJo 10.7.2 (Supplementary Fig. S2).

Live Cell Biotinylated FN Recycling Assay

HCFs were transfected (P3 Primary Cell Solution) with 2 µg of control or USP10 cDNA and replated in DMEM/F-12 and 1% FBS. Twenty-four hours after transfection, the cells were loaded with 10 µg biotinylated FN for 3 hours. The cells were then passaged with trypsin and plated on 35-mm glass-bottom dishes in DMEM/F-12 and 1% FBS. On days 1 to 4, the cells were washed three times for 30 minutes each prior to imaging with the following procedure: 1X PBS with 1% BSA (bovine serum albumin) (PBSA) in PHEM (60-mM PIPES, 25-mM HEPES, 10-mM EGTA, and 4-mM $MgSO_4$); 150-mM sodium azide (Sigma-Aldrich) in PHEM; and 1:100 streptavidin-488 in PHEM. Images were captured on a Zeiss LSM 780 confocal microscope and analyzed using the 3D Object Counter plugin for ImageJ.

Live Cell αv and $\alpha5\beta1$ Blocking Antibody FN Recycling Experiment

HCFs were transfected (P3 Primary Cell Solution) with 2 µg of control or USP10 cDNA and replated in DMEM/F-12 and 1% FBS. Twenty-four hours after transfection, the cells were treated with 10 µg/mL αv and $\alpha5\beta1$ blocking antibodies. After 1 hour, the cells were loaded with biotinylated FN for 3 hours (antibodies remained in the conditioned media, 4 hours total). The cells were then passaged and replated in a 24-well glass-bottom dish. After 48 hours, images were captured on a Zeiss LSM 780 confocal microscope and analyzed using the 3D Object Counter plugin for ImageJ. Cell detachment was not observed with these antibodies with the time point examined.

Live Cell Assay: Percentage of FN-EDA Versus Recycled Biotinylated FN

Cells were transfected with 2 µg of control or USP10 cDNA and replated in DMEM/F-12 and 1% FBS. Twenty-four hours after transfection, the cells were loaded with 10 µg biotinylated FN for 3 hours. Cells were then passaged and replated on a 24-well glass-bottom plate (1812-024; Chemglass, Vineland, NJ, USA). After 48 hours, cells were treated separately with a streptavidin-488 or a FN-EDA-488 (Santa Cruz) antibody to avoid any differences in quantification of fluorophore. Images were captured on a Zeiss LSM 780 confocal microscope and analyzed using the 3D Object Counter plugin for ImageJ.

Image Quantification

Live cell images were captured using a Zeiss LSM 780 confocal microscope with a 40× oil immersion objective. Each image was taken at 212.55 × 212.55 mm (2636 × 2636 pixels) and analyzed using ImageJ. For integrin recycling (Fig. 1), the Analyze Particles plugin for ImageJ was used to threshold the images and measure the percent area of fluorescence of the image. For fibronectin recycling and secreted FN (Figs. 3–5), the 3D Object Counter plugin for ImageJ was used to threshold images and quantify puncta (above 0.01 mm in size).

Statistical Analysis

Graphical data are the mean ± SEM of at least three technical repeats using two different patient-derived cell lines. Statistical significance for analysis of these images was calculated using a Student's *t*-test, one-way ANOVA, and Tukey's multiple comparisons test or two-way ANOVA and Fisher's test.

Results

USP10 Overexpression Increases Integrin Recycling and FN Endocytosis

Previously, we demonstrated by cell surface biotinylation that integrins αv, $\beta1$, and $\beta5$ accumulate on the cell surface of HCFs in response to USP10 overexpression. This resulted from post-translational removal of ubiquitin from integrins.[13] Although it is assumed that reduced degradation in response to less ubiquitination and accumulation on the cell surface indicates that USP10 overexpression promotes integrin recycling instead of degradation, to prove this we subjected HCFs to a live cell confocal integrin recycling assay.

HCFs were transfected with either control or USP10 cDNA and incubated for 48 hours. To quantify $\alpha5\beta1$ and αv recycling to the cell surface, cells were treated with either anti-$\alpha5\beta1$ or anti-αv antibody for 30 minutes at 37°C prior to cell surface stripping with low-pH buffer and another 30-minute incubation at 37°C to allow for recycling of integrins

Investigative Ophthalmology & Visual Science

bound to their respective antibodies.[39] Signal was quantified by detection with secondary antibody-488 and imaged by live cell confocal microscopy so that only external (recycled) integrins were imaged and quantified. We found that USP10 overexpression increased $\alpha 5\beta 1$ integrin recycling by 1.9-fold ($P < 0.001$), and αv integrin recycling by 1.7-fold ($P < 0.01$) (Figs. 1A–1F) as quantified by total fluorescence intensity (see Materials and Methods). We used these same images to analyze cell area. We found that USP10 overexpression increased cell area by 1.52-fold ($P < 0.01$) (Supplementary Fig. S1). We reasoned, however, that the cells were not larger, but that they appeared larger on a two-dimensional surface because of the augmented cell-surface integrin levels and improved cell attachment producing a flatter and larger cell compared with control. To directly test if USP10 overexpression increases cell size in solution, we performed flow cytometry comparing control vector-FLAG transduced cells compared to USP10-FLAG overexpressing cells. We found no difference in the size of the USP10 overexpressing cells compared with control (Supplementary Fig. S2). Furthermore, the fact that biochemical endpoints that are equalized by protein, not microscopic images (western blots and immunoprecipitation of cell-surface integrins),[13] demonstrate a more than two-fold difference in cell-surface integrin accumulation[13] and FN internalization by ELISA (see below) when USP10 is overexpressed supports the idea that USP10 increases cell-surface integrin expression, not simply larger cells.

Because cell-surface integrin expression is increased in USP10 overexpressing cells, and FN is endocytosed via integrins, we next asked if USP10 overexpression increased uptake of FN. HCFs were transfected with USP10 or control cDNA. After 48 hours, cells were loaded with biotinylated FN for 3 hours prior to cell detachment with trypsin and lysing. Samples were equalized by protein concentration. A FN ELISA was used to quantify intracellular biotinylated FN. USP10 overexpressing cells increased FN uptake by 2.2-fold ($P < 0.05$) (Fig. 1G).

Establishing a FN Recycling Assay

We used FN-FITC to test conditions and time points for a FN recycling assay. Although FN recycling assays have been established,[40] our ultimate goal was a quantitative live cell imaging approach. First, to establish the parameters of FN fibril formation, HCFs were incubated for 3 hours with soluble FN-FITC and then fixed and imaged (pre-passage). The remainder of the cells were detached with trypsin, replated, and imaged at 2, 18, 36, and 72 hours post-passage to determine if internalized FN would re-emerge and organize fibrils (Fig. 2A). We found that plating cells in media containing at least 1% FBS was required to produce consistent fibril

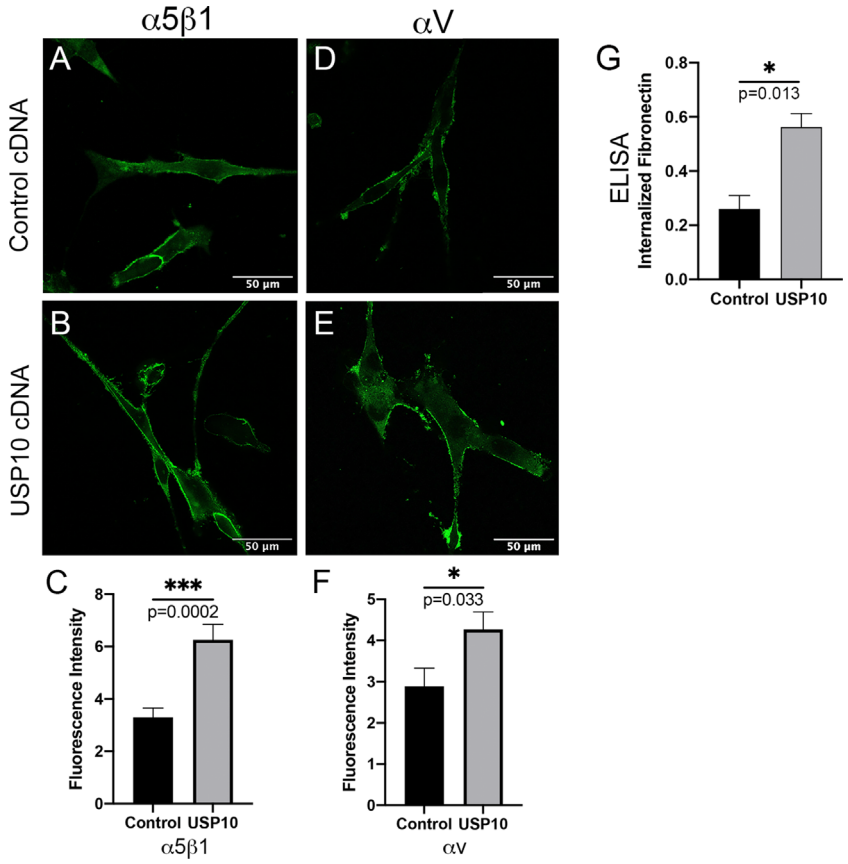

Figure 1. USP10 overexpression promoted integrin recycling and fibronectin endocytosis. (**A–F**) Live cell integrin recycling assay. HCFs were transfected with 2ug control or USP10 cDNA. 48 hours post transfection, integrin recycling was detected with anti-rabbit-488 antibody prior to imaging by live cell confocal microscopy. *Scale bar*: 50 µm. (**C**) Fluorescence intensity of $\alpha 5\beta 1$ integrin recycling fold change (1.9; $P < 0.001$) and (**F**) αv (1.7; $P < 0.05$) when USP10 was overexpressed. (**G**) FN ELISA. HCFs were transfected with 2 µg control or USP10 cDNA. Twenty-four hours after transfection, HCFs were loaded with biotinylated FN for 3 hours prior to detachment and lysing. Endocytosed FN was quantified with the Quantikine ELISA kit. USP10 overexpression induced an increase internalized fibronectin fold change (2.1; $P < 0.05$, Student's *t*-test). Two primary cell lines (total $N = 3$ repeats). Five images per condition/per experiment were analyzed.

Investigative Ophthalmology & Visual Science

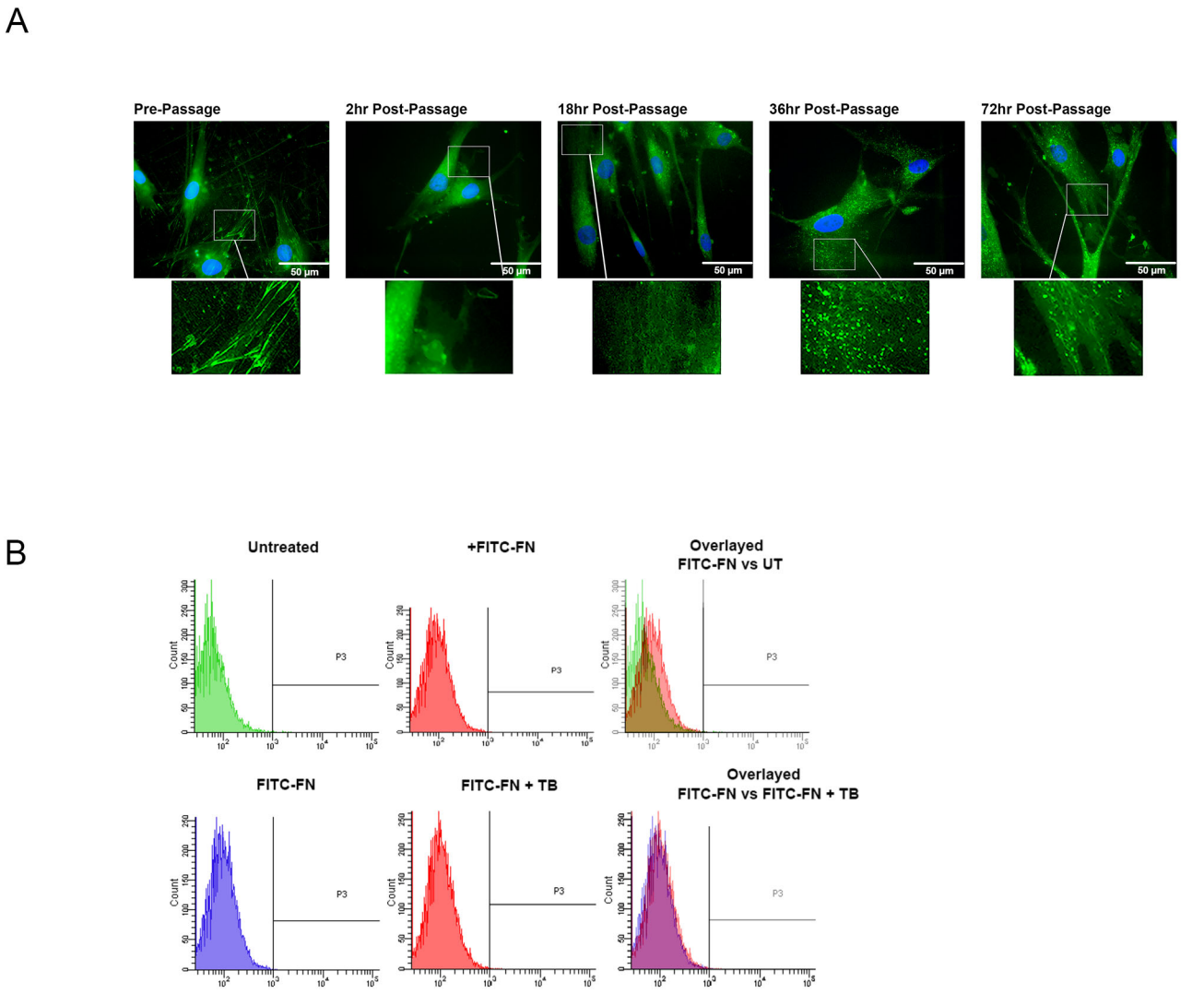

Figure 2. Extracellular FN was removed by trypsinization. (**A**) To determine if soluble FN would form fibrils in our assay conditions, HCFs were loaded with FN-FITC for 90 minutes. Cells were imaged immediately or were passaged with trypsin and then replated and imaged at the corresponding time points. (**B**) Flow cytometry was utilized to determine if cell passaging was sufficient to remove extracellular FN. HCFs were loaded with FN-FITC for 90 minutes. (*Top row*) Untreated cells compared with FN-FITC treated cells and overlay. (*Bottom row*) Extracellular fluorescence was quenched with Trypan Blue. FN-FITC–treated cells compared with the FN-FITC + Trypan Blue (TB)–treated cells and overlay. Two primary cell lines (total $N = 3$ repeats).

organization. Organized dots were observed by 36 hours, and by 72 hours fibrils were forming (arrows). Because the cells were fixed and FN-FITC was used in this assay, we cannot distinguish between intracellular and extracellular FN-FITC. However, we used FN-FITC to easily detect fibril formation and to enable detection by flow cytometry for the next step—to prove that trypsin removes all extracellular FN-FITC from the cell surface.

HCFs were incubated without FN-FITC (control) or with FN-FITC for 3 hours prior to trypsinization. Pelleted cells were subjected to flow cytometry. The data in the top row of Figure 2B demonstrate that, compared to control, the FN-FITC–treated cells had an increased signal, and cells were shifted to the right. In the second set of experiments, FN-FITC–treated cells were trypsinized, pelleted, and treated with or without Trypan Blue. Trypan Blue masks the FITC extracellular signal.[41] FN-FITC–treated cells compared with FN-FITC–treated cells with Trypan Blue presented with identical profiles, demonstrating that the FITC signal is intracellular and that, as expected, the trypsin had removed extracellular FN-FITC (Fig. 2B, bottom row). Together these data suggest that internalized FN can produce extracellular fibrils in the time frame tested and that trypsin can reliably remove extracellular FN.

USP10 Overexpression Increases Extracellular FN Expression and Organization

Using the parameters discovered in the above assays, we utilized soluble biotinylated FN and live cell imaging to detect extracellular fibrillar biotinylated FN. HCFs were transfected with either control or USP10 cDNA. After 24 hours, cells were loaded for 3 hours with biotinylated FN, trypsinized, and replated for live cell imaging. At days 1 to 4 after reseeding, biotinylated FN was detected with streptavidin-488. Because the cells were neither fixed nor permeabilized, only the extracellular biotinylated FN was

Investigative Ophthalmology & Visual Science

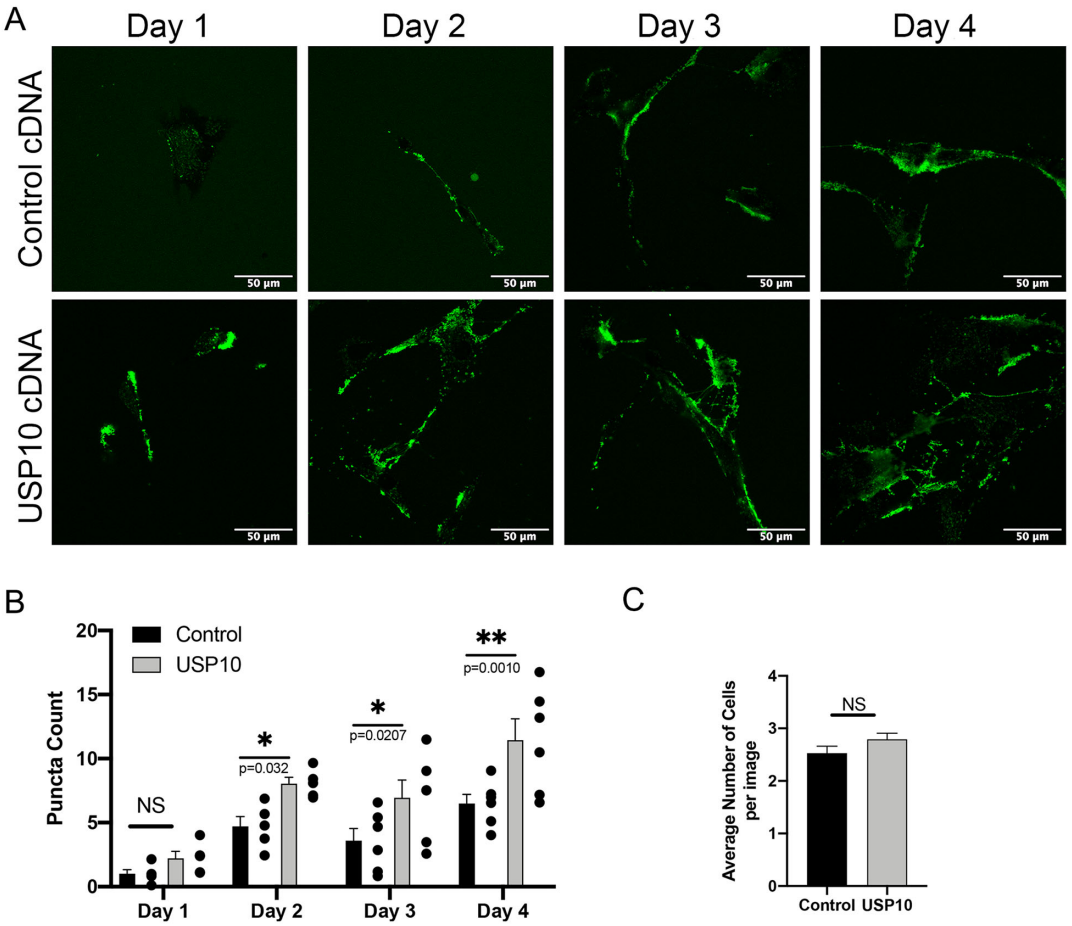

Figure 3. USP10 overexpression increased FN recycling. For the live cell FN recycling assay, HCFs were transfected with 2 µg control or USP10 cDNA. Twenty-four hours after transfection, HCFs were loaded with biotinylated FN for 3 hours. After trypsinization, cells were replated for days 1 to 4. FN recycling was detected with streptavidin-488 by live cell confocal microscopy. (**A**) Images from days 1 to 4. *Scale bar*: 50 µm. (**B**) Quantification of puncta count; USP10 overexpressing cells increased FN recycling (1.7–2.2-fold). Two-way ANOVA, two primary cell lines, total $N = 6$ repeats, five images per condition/per experiment. One *dot* represents the average of quantification of images in one experiment. (**C**) Average number of cells quantified per image were similar; Student's *t*-test.

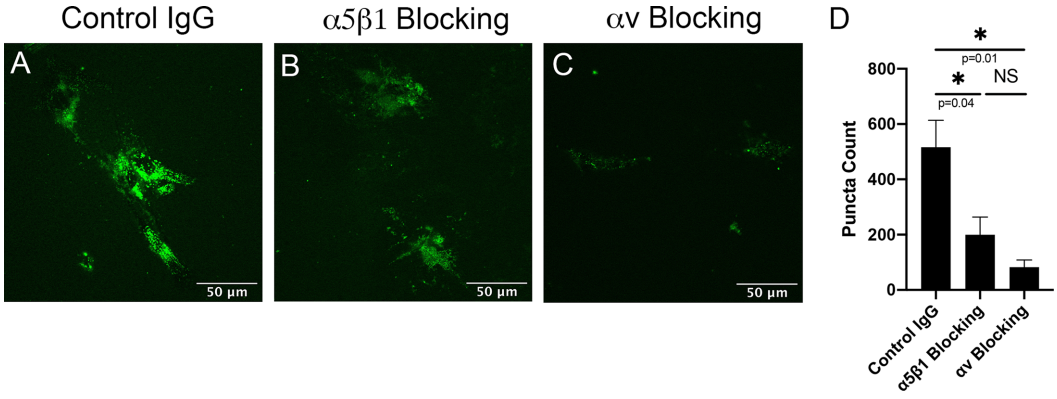

Figure 4. Blocking integrins reduced FN recycling. (**A–C**) Live cell FN recycling assay. HCFs were transfected with 2 µg USP10 cDNA for 24 hours prior to treatment with control IgG, $\alpha5\beta1$ integrin-blocking antibody, or αv integrin-blocking antibody. After 1 hour with antibodies, cells were treated with biotinylated FN for 3 hours prior to trypsinization and replating for 2 days. *Scale bar*: 50 µm. (**D**) Quantification. USP10 overexpressing cells treated with control IgG compared with $\alpha5\beta1$ blocking antibody reduced FN recycling by 62% ($P < 0.05$), and IgG compared with αv blocking antibody reduced FN recycling by 84% ($P < 0.05$). One-way ANOVA, two primary cell lines, total $N = 4$ repeats, five images per condition/per experiment were analyzed.

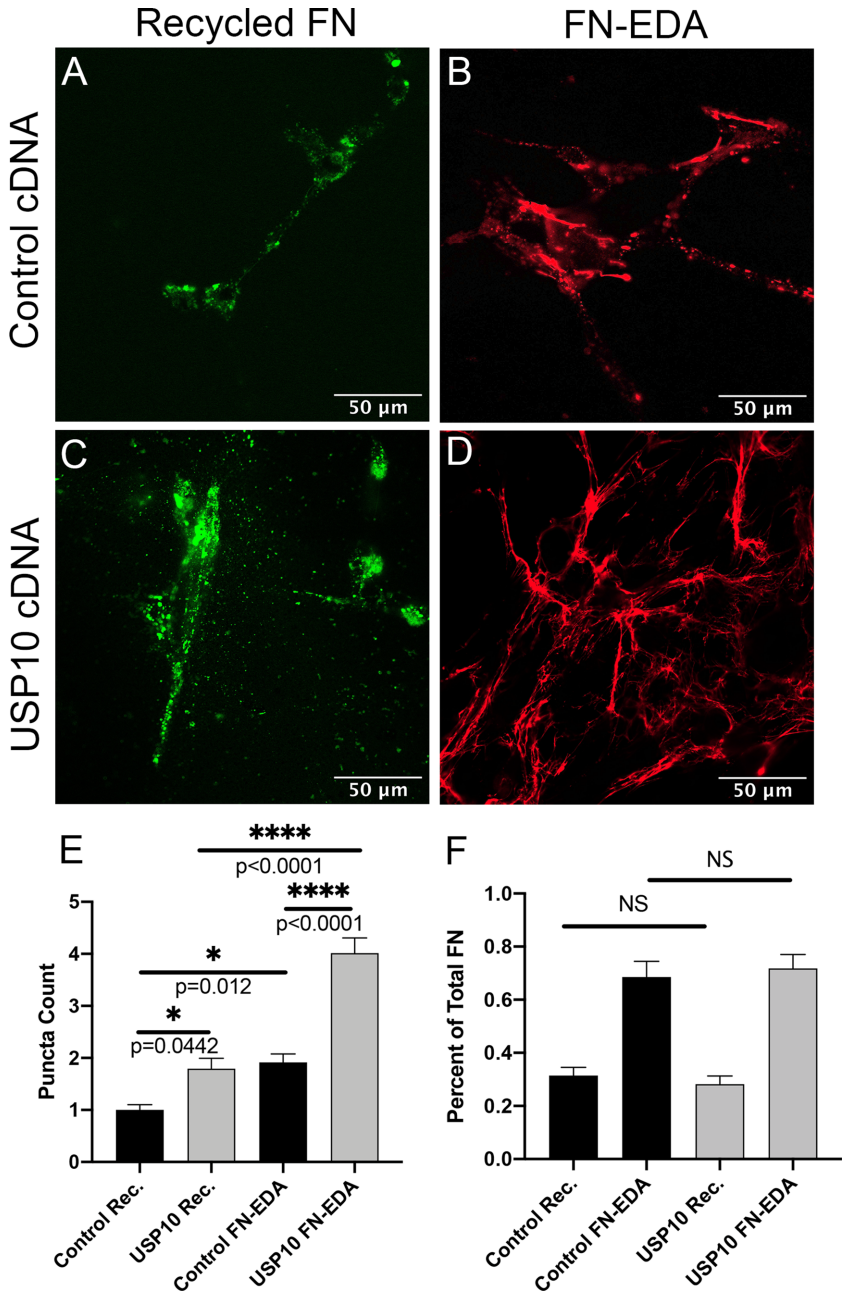

Figure 5. Ratio of total versus recycled FN for live cell FN recycling/secretion assay. (**A**–**D**) HCFs were transfected with 2 µg control or USP10 cDNA. Twenty-four hours after transfection HCFs were loaded with biotinylated FN for 3 hours. After trypsinization, cells were replated for 2 days. (**A**, **C**) FN recycling was detected with streptavidin-488 by live cell confocal microscopy. (**B**, **D**) Secreted FN-EDA was detected with FN-EDA-488 (colored *red* for image). *Scale bars*: 50 µm. (**E**) Quantification of recycled FN in control cells compared with USP10 overexpressing cells (1.79-fold; $P < 0.05$). Quantification of secreted FN-EDA in control cells compared with USP10 overexpressing cells (2.18-fold; $P < 0.05$). (**F**) The percentage of recycled FN and secreted FN-EDA for control cells versus USP10 overexpressing cells was not significantly different. One-way ANOVA, two primary cell lines, total $N = 4$ repeats, five images per condition/per experiment were analyzed.

detected. In Figure 3A shows representative images from days 1 to 4 after reseeding of cells. Images were quantified by puncta count (see Materials and Methods). Using two-way ANOVA, the data from six independent experiments demonstrate that overexpression of USP10 resulted in a (1.7–2.2-fold; $P < 0.05$) increase in extracellular recycled biotinylated FN over a 4-day period (Fig. 3B). The average number of cells in each frame analyzed was not significantly different between conditions (Fig. 3C). To test if USP10 affected total cell number, in separate experiments from the recycling assays cells were counted after transfection from days 1 to 4. In Supplementary Figure S3, we demonstrate that the USP10 cDNA did slightly impact cell viability, although it was not statistically significant. However, comparing the growth rate of cells in each group, USP10 overexpressing cells had a slightly higher growth rate over the 4 days, likely to overcome the cell loss after transfection, but again not statistically significant. These controls demonstrate that the USP10-mediated increase in recycled FN is not derived from a significant overall increase in cell number.

Investigative Ophthalmology & Visual Science

Blocking Integrins Significantly Reduces FN Recycling

To prove that integrins are involved in the recycling of FN, the recycling assay with control or USP10 cDNA was performed as above. Twenty-four hours after transfection, blocking antibodies to either $\alpha5\beta1$ or αv integrin were added 1 hour prior to treatment with biotinylated FN for 3 hours. Cells were trypsinized, reseeded, and analyzed 48 hours later (Fig. 3, day 2). Figure 4 demonstrates a 62% decrease ($P < 0.05$) in FN recycling with $\alpha5\beta1$-blocking antibody and an 84% decrease ($P < 0.05$) with αv-blocking antibody compared with IgG control. Cell detachment was not observed with any of the antibodies in the timeframe of the assay. These data demonstrate that, as expected, FN receptor integrins are involved in FN recycling.

Recycled FN Accounts for Approximately One-Third of Total FN in HCFs

To ascertain the contribution of recycled biotinylated FN compared with cellular FN-EDA, we again overexpressed control or USP10 cDNA in HCFs. After 24 hours, cells were loaded with biotinylated FN for 3 hours and then reseeded for another 48 hours (Fig. 3, day 2). Imaging of biotinylated FN with streptavin-488 was performed on one set of coverslips and compared with cells from the same experiment treated with anti–FN-EDA-488 antibody. Both were imaged by live cell confocal microscopy. Quantifying the recycled FN and FN-EDA separately but each with a 488 fluorophore eliminated any variance between fluorophores during quantification. Representative images from each condition are shown in Figures 5A to 5D. FN-EDA expression is colored red to easily distinguish recycled from endogenously secreted FN. Image analysis is shown in Figure 5E. When control cDNA was compared with USP10 cDNA for recycled FN (Figs. 5A, 5C), we found a 1.8-fold increase in USP10-mediated recycling ($P < 0.05$) (Fig. 3). When control cDNA was compared to USP10 cDNA for extracellular FN-EDA (Figs. 5B, 5D), a 2.1-fold increase in USP10-mediated FN-EDA synthesis and extracellular organization was quantified ($P < 0.0001$). We then calculated the percentage of recycled FN versus secreted FN-EDA in each condition and found that, in HCFs transfected with control cDNA, recycled FN accounted for 34% ± 7% of total and FN-EDA 66% ± 4% of total. Similarly, with USP10 overexpression, recycled FN accounted for 29% ± 5% of total and endogenously secreted FN-EDA 71% ± 9% of total. These percentages are represented in Figure 5F. Interestingly, even though USP10 increased both recycled FN and secreted FN-EDA and therefore the total FN, the relative ratios of recycled and FN-EDA between control and USP10 cDNA were not significantly different.

Discussion

Our previous work on USP10 established that USP10 gene expression is upregulated upon wounding and that USP10 removes ubiquitin from substrate integrins, reducing integrin degradation and initiating an increase in cell-surface integrin accumulation that promotes scarring.[13,22] Furthermore, the subsequent cell-surface integrin–mediated activation of TGFβ induced the myofibroblast phenotype and a significant increase in FN-EDA gene and protein expression and organization, as determined by quantitative PCR, microscopy, and western blot.[13] These results were bolstered by our recent studies demonstrating that knockdown of USP10 after wounding, ex vivo in porcine cornea and in vivo in rabbit corneas, significantly reduced scarring.[13,21,22]

Because integrins are endocytosed with matrix, here we extended our previous studies by testing if reduced intracellular degradation of integrins as a result of USP10 overexpression (USP10 removes ubiquitin, integrins accumulate) would also result in USP10-driven matrix accumulation if integrin/ECM were recycled back to the cell surface together. We focused on integrins $\alpha5\beta1$ and αv and the matrix molecule FN, which undergoes a stepwise integrin-dependent polymerization to generate fibrils from soluble, monomeric FN.[42–45] The $\alpha5\beta1$ and αv integrins recognize the common integrin-binding motif (RGD) in FN[25,46,47] and coordinate to achieve efficient FN binding.[26,48]

We found that USP10 overexpression increased αv and $\alpha5\beta1$ integrin recycling, FN uptake, and FN recycling (Figs. 1–4). Furthermore, FN-EDA secretion was also significantly increased, as previously reported to result from elevated USP10-induced integrin-mediated TGFβ activity.[13] We found here that the relative contributions of endogenously secreted FN-EDA compared with recycled FN were approximately 2/3 to 1/3 of total FN, respectively (Fig. 5). An overview of these USP10-mediated integrin/FN findings are diagrammed in Figure 6.

Our recycling and secretion experiments were performed in media containing 1% serum, which we found was necessary to generate observable fibril formation in the timeframe of 1 to 4 days. We cannot totally discount the possible contribution of serum-derived FN-EDA to the FN matrix that we detected as endogenously secreted FN (Fig. 5, red) or the contribution of serum-containing factors to the stimulation of endogenous synthesis of FN-EDA. However, overall, FN in serum is largely plasma FN and not cellular FN (FN-EDA), and plasma FN will not be detected with the FN-EDA–specific antibody. Also, importantly, as one would expect, the same media were used in both control and USP10 overexpressing cells. Thus, any cross-reactivity of the anti–FN-EDA to FN or serum-derived growth factor–mediated stimulation of FN-EDA would be detected equally in both control and USP10 overexpressing cells. Furthermore, the finding that in 1% serum-containing media we still observed a greater than two-fold increase in endogenously secreted FN-EDA in USP10 overexpressing cells (similar to our data in serum-free media)[13] suggests that the 1% serum-containing media did not obscure results. In addition, we used a 488 fluorophore to detect both recycled and secreted FN on cells from the same transfection experiment but in parallel, instead of double labeling with two different fluorophores. We did this to eliminate any differences in quantification between two different fluorophores. The secreted FN-EDA was assigned a red color in Figure 5 to differentiate between the two FNs. Together, our data support a largely unappreciated contribution of integrin-mediated recycled FN to the accumulation of ECM in fibrosis. Furthermore, the deubiquitinase USP10 modulates integrin/FN recycling and cell surface accumulation.

Mechanistically, endocytosis of FN is linked to fibrotic phenotypes. Fibrillar FN is cleaved by MT1-MMP, endocytosed in an integrin and caveolin-1–dependent manner, and degraded in the lysosome.[28,29] A previous study demonstrated that $\alpha5\beta1$ binding to FN was necessary for ubiquitination of $\alpha5$ and degradation of the internalized $\alpha5\beta1$/FN complex in the endosomal pathway. Furthermore,

Investigative Ophthalmology & Visual Science

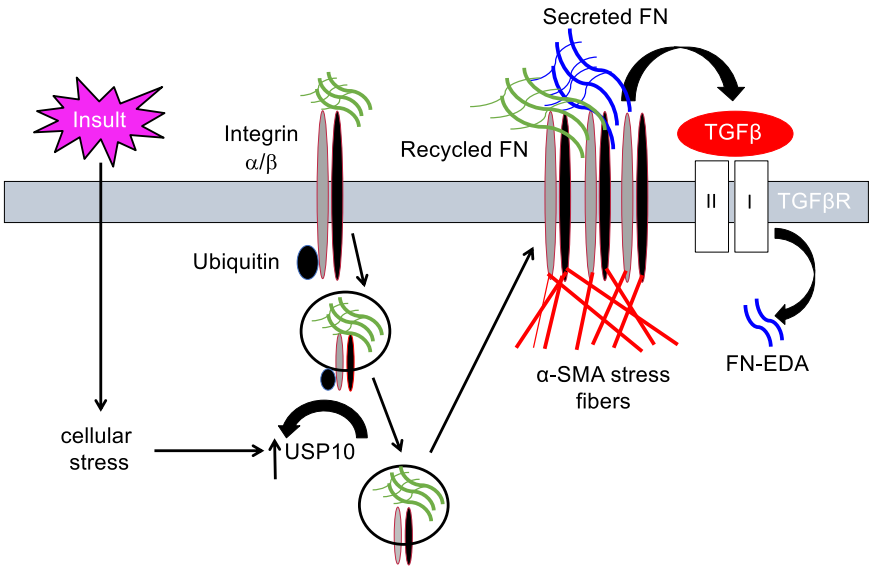

Figure 6. Working model for USP10-mediated matrix deposition during wound healing Wounding initiates cell stress pathways. USP10 expression is increased after wounding, reducing integrin degradation through ubiquitin removal.[13,22] This shift promotes integrin recycling to the cell surface with endocytosed matrix (*green*). The increase in USP10-mediated integrin accumulation also leads to activation of TGFβ signaling, inducing FN-EDA secretion (*blue*) and the organization of α-SMA–containing stress fibers (*red*).[13]

degradation of the complex was necessary for cell migration.[49] The authors proposed that reduced degradation of integrins would instead induce recycling of the complex to the cell surface to form dysfunctional adhesion sites yielding pathological cell adhesion and a buildup of ECM. In support of this idea, a recent study found that, in response to exogenous TGFβ treatment, endocytosed FN favored recycling through a rab11 pathway back to the cell surface over intracellular degradation, with a requirement for TGFβRII binding to $\alpha5\beta1$.[30] Similarly, we found that USP10 overexpression (which induces TGFβ activity)[4] increased integrin recycling (Figs. 1A–1F), FN endocytosis (Fig. 1G), and FN recycling (Fig. 3).

The connection between DUBs and fibrosis is a burgeoning field.[50] The DUB ubiquitin C-terminal hydrolase L1 (UCH-L1) is suggested to play a role in liver fibrosis, as knockdown of UCH-L1 blocks progression of CCl_4-induced fibrosis in mice, and a specific UCH-L1 inhibitor blocks fibrosis in a cellular idiopathic pulmonary fibrosis model.[51,52] DUBs also have been found to directly regulate TGFβ signaling. UCH-L5 stabilizes SMAD2/3, and USP11 stabilizes TGFβ receptor TβRII, promoting TGFβ1 signaling. Both DUBs were also increased in patients with idiopathic pulmonary fibrosis and bleomycin-challenged mice.[53,54] Furthermore, pan-inhibition of DUBs with the DUB inhibitor PR-619 ameliorates renal fibrosis through the SMAD4 pathway.[55] Finally, in a model of diabetic renal fibrosis, the DUB ubiquitin-specific peptidase 9 X-linked (USP9X) is protective, attenuating advanced glycation-end products and subsequent fibrotic markers.[56]

In terms of the biological and pathological importance of cellular FN-EDA, studies have linked this splice variant to the generation of fibrotic outcomes in many tissues.[57,58] FN-EDA expression is downstream of PI3K/AKT signaling.[59,60] There are several pathways of AKT activation leading to subsequent FN-EDA expression. β1-integrin activation leads to the phosphorylation of focal adhesion kinase (FAK) on Tyr-397 and in turn, PI3K and AKT activation.[61] Other studies have shown that TGFβ can activate FAK through a Smad3 pathway or activate PI3K/AKT through a p38 pathway.[60] Regardless of the upstream events, AKT activation leads to FN-EDA expression and myofibroblast persistence[59,60] Recently, it was discovered that FN-EDA binds preferentially to the latent TGFβ protein binding protein 1 (LTBP-1), and blocking this interaction results in reduced local TGFβ activity.[32] Supporting the idea that FN-EDA is critical to TGFβ signaling is the finding that FN-EDA null mice display dysfunctional healing but are protected against bleomycin-induced lung fibrosis.[58,62,63] In addition, lung cancer cell–secreted FN-EDA binds to monocytes driving proinflammatory responses in the tumor microenvironment via the nuclear factor-κB (NF-κB) pathway, and circulating FN-EDA was found to be a biomarker for endothelial cell activation and inflammation in diabetes.[64–66] Because of the importance of matrix to disease and pathologies, it is thought that standard therapies are in part effective because of their secondary effect on ECM. New therapies are directly targeting ECM, and ECM ligands are also being used as drug delivery mechanisms.[67–70] Because integrin/ECM binding and accumulation play a central role in pathological myofibroblast persistence, USP10 may be an important new target for anti-scarring therapy. Overall, our work demonstrates that DUB-mediated intracellular control of integrin trafficking is a novel method to regulate cell surface accumulation of recycled integrins with their corresponding ECM.

Acknowledgments

Supported by grants from the National Eye Institute, National Institutes of Health (R01 EY024942, R01 EY030567), US Department of Veteran's Affairs Biomedical Laboratory Research and Development Service Merit Review Award (I01 BX005360), SUNY Upstate Start-Up Funds, unrestricted grant to the Department of Ophthalmology and Visual Sciences from Research to Prevent Blindness and Lions Club District 20-Y (AMB), Charles H. Best foundation fellowship (EG), an operating grant from the

Canadian Institutes of Health Research (MOP-136944), and an operating grant from Bristol-Myers Squibb (SSS).

Disclosure: **A.T. Phillips**, None; **E.F. Boumil**, None; **N. Castro**, None; **A. Venkatesan**, None; **E. Gallo**, None; **J.J. Adams**, None; **S.S. Sidhu**, None; **A.M. Bernstein**, None

References

1. Whitcher JP, Srinivasan M, Upadhyay MP. Corneal blindness: a global perspective. *Bull World Health Organ*. 2001;79:214–221.
2. Stepp MA, Zieske JD, Trinkaus-Randall V, et al. Wounding the cornea to learn how it heals. *Exp Eye Res*. 2014;121:178–193.
3. Barrientez B, Nicholas SE, Whelchel A, Sharif R, Hjortdal J, Karamichos D. Corneal injury: clinical and molecular aspects. *Exp Eye Res*. 2019;186:107709.
4. Wilson SE, Sampaio LP, Shiju TM, Carlos de Oliveira R. Fibroblastic and bone marrow-derived cellularity in the corneal stroma. *Exp Eye Res*. 2021;202:108303.
5. Wilson SE. Corneal myofibroblasts and fibrosis. *Exp Eye Res*. 2020;201:108272.
6. Pakshir P, Noskovicova N, Lodyga M, et al. The myofibroblast at a glance. *J Cell Sci*. 2020;133:jcs227900.
7. Wilson SE, Chaurasia SS, Medeiros FW. Apoptosis in the initiation, modulation and termination of the corneal wound healing response. *Exp Eye Res*. 2007;85:305–311.
8. Parapuram SK, Hodge W. The integrin needle in the stromal haystack: emerging role in corneal physiology and pathology. *J Cell Commun Signal*. 2014;8:113–124.
9. Leask A. Integrin 1: a mechanosignaling sensor essential for connective tissue deposition by fibroblasts. *Adv Wound Care (New Rochelle)*. 2013;2:160–166.
10. Hinz B. The extracellular matrix and transforming growth factor-β1: tale of a strained relationship. *Matrix Biol*. 2015;47:54–65.
11. Wipff PJ, Rifkin DB, Meister JJ, Hinz B. Myofibroblast contraction activates latent TGF-beta1 from the extracellular matrix. *J Cell Biol*. 2007;179:1311–1323.
12. Wang L, Pedroja BS, Meyers EE, Garcia AL, Twining SS, Bernstein AM. Degradation of internalized αvβ5 integrin is controlled by uPAR bound uPA: effect on β1 integrin activity and α-SMA stress fiber assembly. *PLoS One*. 2012;7:e33915.
13. Gillespie SR, Tedesco LJ, Wang L, Bernstein AM. The deubiquitylase USP10 regulates integrin β1 and β5 and fibrotic wound healing. *J Cell Sci*. 2017;130:3481–3495.
14. Henderson NC, Arnold TD, Katamura Y, et al. Targeting of αv integrin identifies a core molecular pathway that regulates fibrosis in several organs. *Nat Med*. 2013;19:1617–1624.
15. Reed NI, Jo H, Chen C, et al. The αvβ1 integrin plays a critical in vivo role in tissue fibrosis. *Sci Transl Med*. 2015;7:288ra279.
16. Conroy KP, Kitto LJ, Henderson NC. αv integrins: key regulators of tissue fibrosis. *Cell Tissue Res*. 2016;365:511–519.
17. Henderson NC, Rieder F, Wynn TA. Fibrosis: from mechanisms to medicines. *Nature*. 2020;587:555–566.
18. Eldred JA, Dawes LJ, Wormstone IM. The lens as a model for fibrotic disease. *Philos Trans R Soc Lond B Biol Sci*. 2011;366:1301–1319.
19. Lobert VH, Stenmark H. Ubiquitination of α-integrin cytoplasmic tails. *Commun Integr Biol*. 2010;3:583–585.
20. Hsia HC, Nair MR, Corbett SA. The fate of internalized α5 integrin is regulated by matrix-capable fibronectin. *J Surg Res*. 2014;191:268–279.
21. Castro N, Gillespie SR, Bernstein AM. Ex vivo corneal organ culture model for wound healing studies. *J Vis Exp*. 2019;144:10.3791/58562.
22. Boumil EF, Castro N, Phillips AT, et al. USP10 targeted self-deliverable siRNA to prevent scarring in the cornea. *Mol Ther Nucleic Acids*. 2020;21:1029–1043.
23. Sechler JL, Takada Y, Schwarzbauer JE. Altered rate of fibronectin matrix assembly by deletion of the first type III repeats. *J Cell Biol*. 1996;134:573–583.
24. Wierzbicka-Patynowski I, Schwarzbauer JE. The ins and outs of fibronectin matrix assembly. *J Cell Sci*. 2003;116:3269–3276.
25. Benito-Jardon M, Strohmeyer N, Ortega-Sanchis S, et al. αv-Class integrin binding to fibronectin is solely mediated by RGD and unaffected by an RGE mutation. *J Cell Biol*. 2020;219:e202004198.
26. Bharadwaj M, Strohmeyer N, Colo GP, et al. αV-class integrins exert dual roles on α5β1 integrins to strengthen adhesion to fibronectin. *Nat Commun*. 2017;8:14348.
27. Shi F, Sottile J. Caveolin-1-dependent β1 integrin endocytosis is a critical regulator of fibronectin turnover. *J Cell Sci*. 2008;121:2360–2371.
28. Sottile J, Chandler J. Fibronectin matrix turnover occurs through a caveolin-1-dependent process. *Mol Biol Cell*. 2005;16:757–768.
29. Shi F, Sottile J. MT1-MMP regulates the turnover and endocytosis of extracellular matrix fibronectin. *J Cell Sci*. 2011;124:4039–4050.
30. Varadaraj A, Jenkins LM, Singh P, et al. TGF-β triggers rapid fibrillogenesis via a novel TβRII-dependent fibronectin-trafficking mechanism. *Mol Biol Cell*. 2017;28:1195–1207.
31. Mana G, Clapero F, Panieri E, et al. PPFIA1 drives active α5β1 integrin recycling and controls fibronectin fibrillogenesis and vascular morphogenesis. *Nat Commun*. 2016;7:13546.
32. Klingberg F, Chau G, Walraven M, et al. The fibronectin ED-A domain enhances recruitment of latent TGF-β-binding protein-1 to the fibroblast matrix. *J Cell Sci*. 2018;131:jcs201293.
33. Valiente-Alandi I, Potter SJ, Salvador AM, et al. Inhibiting fibronectin attenuates fibrosis and improves cardiac function in a model of heart failure. *Circulation*. 2018;138:1236–1252.
34. Altrock E, Sens C, Wuerfel C, et al. Inhibition of fibronectin deposition improves experimental liver fibrosis. *J Hepatol*. 2015;62:625–633.
35. Filla MS, Faralli JA, Desikan H, Peotter JL, Wannow AC, Peters DM. Activation of αvβ3 integrin alters fibronectin fibril formation in human trabecular meshwork cells in a ROCK-independent manner. *Invest Ophthalmol Vis Sci*. 2019;60:3897–3913.
36. Faralli JA, Filla MS, McDowell CM, Peters DM. Disruption of fibronectin fibrillogenesis affects intraocular pressure (IOP) in BALB/cJ mice. *PLoS One*. 2020;15:e0237932.
37. Bowers SLK, Davis-Rodriguez S, Thomas ZM, et al. Inhibition of fibronectin polymerization alleviates kidney injury due to ischemia-reperfusion. *Am J Physiol Renal Physiol*. 2019;316:F1293–F1298.
38. Bhattacharyya S, Tamaki Z, Wang W, et al. FibronectinEDA promotes chronic cutaneous fibrosis through Toll-like receptor signaling. *Sci Transl Med*. 2014;6:232ra250.
39. Ubelmann F, Burrinha T, Salavessa L, et al. Bin1 and CD2AP polarise the endocytic generation of beta-amyloid. *EMBO Rep*. 2017;18:102–122.
40. Varadaraj A, Magdaleno C, Mythreye K. Deoxycholate fractionation of fibronectin (FN) and biotinylation assay to measure recycled FN fibrils in epithelial cells. *Bio Protoc*. 2018;8:e2972.
41. Illien F, Rodriguez N, Amoura M, et al. Quantitative fluorescence spectroscopy and flow cytometry analyses of cell-penetrating peptides internalization pathways:

optimization, pitfalls, comparison with mass spectrometry quantification. *Sci Rep*. 2016;6:36938.
42. Wierzbicka-Patynowski I, Mao Y, Schwarzbauer JE. Analysis of fibronectin matrix assembly. *Curr Protoc Cell Biol*. 2004;Chapter 10:Unit 10.12.
43. Mao Y, Schwarzbauer JE. Fibronectin fibrillogenesis, a cell-mediated matrix assembly process. *Matrix Biol*. 2005;24:389–399.
44. Schwarzbauer JE, Sechler JL. Fibronectin fibrillogenesis: a paradigm for extracellular matrix assembly. *Curr Opin Cell Biol*. 1999;11:622–627.
45. Pankov R, Momchilova A, Stefanova N, Yamada KM. Characterization of stitch adhesions: fibronectin-containing cell-cell contacts formed by fibroblasts. *Exp Cell Res*. 2019;384:111616.
46. Huveneers S, Truong H, Fassler R, Sonnenberg A, Danen EH. Binding of soluble fibronectin to integrin alpha5 beta1 - link to focal adhesion redistribution and contractile shape. *J Cell Sci*. 2008;121:2452–2462.
47. Danen EH, Sonnenberg A. Integrins in regulation of tissue development and function. *J Pathol*. 2003;200:471–480.
48. Benito-Jardon M, Strohmeyer N, Otega-Sanchis S, et al. Correction: αv-class integrin binding to fibronectin is solely mediated by RGD and unaffected by an RGE mutation. *J Cell Biol*. 2021;220:jcb.20200419812072020c.
49. Lobert VH, Brech A, Pedersen NM, et al. Ubiquitination of alpha 5 beta 1 integrin controls fibroblast migration through lysosomal degradation of fibronectin-integrin complexes. *Dev Cell*. 2010;19:148–159.
50. Li S, Zhao J, Shang D, Kass DJ, Zhao Y. Ubiquitination and deubiquitination emerge as players in idiopathic pulmonary fibrosis pathogenesis and treatment. *JCI Insight*. 2018;3:e120362.
51. Wilson CL, Murphy LB, Leslie J, et al. Ubiquitin C-terminal hydrolase 1: a novel functional marker for liver myofibroblasts and a therapeutic target in chronic liver disease. *J Hepatol*. 2015;63:1421–1428.
52. Panyain N, Godinat A, Lanyon-Hogg T, et al. Discovery of a potent and selective covalent inhibitor and activity-based probe for the deubiquitylating enzyme UCHL1, with antifibrotic activity. *J Am Chem Soc*. 2020;142:12020–12026.
53. Nan L, Jacko AM, Tan J, et al. Ubiquitin carboxyl-terminal hydrolase-L5 promotes TGFβ-1 signaling by deubiquitinating and stabilizing Smad2/Smad3 in pulmonary fibrosis. *Sci Rep*. 2016;6:33116.
54. Jacko AM, Nan L, Li S, et al. De-ubiquitinating enzyme, USP11, promotes transforming growth factor β-1 signaling through stabilization of transforming growth factor β receptor II. *Cell Death Dis*. 2016;7:e2474.
55. Soji K, Doi S, Nakashima A, Sasaki K, Doi T, Masaki T. Deubiquitinase inhibitor PR-619 reduces Smad4 expression and suppresses renal fibrosis in mice with unilateral ureteral obstruction. *PLoS One*. 2018;13:e0202409.
56. Huang K, Zhao X. USP9X prevents AGEs-induced upregulation of FN and TGF-β1 through activating Nrf2-ARE pathway in rat glomerular mesangial cells. *Exp Cell Res*. 2020;393:112100.
57. Miller CG, Budoff G, Prenner JL, Schwarzbauer JE. Minireview: fibronectin in retinal disease. *Exp Biol Med (Maywood)*. 2017;242:1–7.
58. Zent J, Guo LW. Signaling mechanisms of myofibroblastic activation: outside-in and inside-out. *Cell Physiol Biochem*. 2018;49:848–868.
59. Abdalla M, Goc A, Segar L, Somanath PR. Akt1 mediates α-smooth muscle actin expression and myofibroblast differentiation via myocardin and serum response factor. *J Biol Chem*. 2013;288:33483–33493.
60. Horowitz JC, Rogers DS, Sharma V, et al. Combinatorial activation of FAK and AKT by transforming growth factor-beta1 confers an anoikis-resistant phenotype to myofibroblasts. *Cell Signal*. 2007;19:761–771.
61. Xia H, Nho RS, Kahm J, Kleidon J, Henke CA. Focal adhesion kinase is upstream of phosphatidylinositol 3-kinase/Akt in regulating fibroblast survival in response to contraction of type I collagen matrices via a beta 1 integrin viability signaling pathway. *J Biol Chem*. 2004;279:33024–33034.
62. Muro AF, Chauhan AK, Gajovic S, et al. Regulated splicing of the fibronectin EDA exon is essential for proper skin wound healing and normal lifespan. *J Cell Biol*. 2003;162:149–160.
63. Muro AF, Moretti FA, Moore BB, et al. An essential role for fibronectin extra type III domain A in pulmonary fibrosis. *Am J Respir Crit Care Med*. 2008;177:638–645.
64. Rajak S, Hussain Y, Singh K, et al. Cellular fibronectin containing extra domain A causes insulin resistance via Toll-like receptor 4. *Sci Rep*. 2020;10:9102.
65. Amin A, Mokhdomi TA, Bukhari S, et al. Lung cancer cell-derived EDA-containing fibronectin induces an inflammatory response from monocytes and promotes metastatic tumor microenvironment. *J Cell Biochem*. 2021;122:562–576.
66. McKeown-Longo PJ, Hyaluronan Higgins PJ., Transforming growth factor β, and extra domain A-fibronectin: a fibrotic triad. *Adv Wound Care (New Rochelle)*. 2021;10:137–152.
67. Jarvelainen H, Sainio A, Koulu M, Wight TN, Penttinen R. Extracellular matrix molecules: potential targets in pharmacotherapy. *Pharmacol Rev*. 2009;61:198–223.
68. Hwang J, Sullivan MO, Kiick KL. Targeted drug delivery via the use of ECM-mimetic materials. *Front Bioeng Biotechnol*. 2020;8:69.
69. Nishida T, Inui M, Nomizu M. Peptide therapies for ocular surface disturbances based on fibronectin-integrin interactions. *Prog Retin Eye Res*. 2015;47:38–63.
70. Ahmad V. Prospective of extracellular matrix and drug correlations in disease management. *Asian J Pharm Sci*. 2020;16:147–160.
71. Ricart AD, Tolcher AW, Liu G, et al. Volociximab, a chimeric monoclonal antibody that specifically binds alpha5beta1 integrin: a phase I, pharmacokinetic, and biological correlative study. *Clin Cancer Res*. 2008;14:7924–7929.
72. Li L, Hu X, Eid JE, et al. Mutant IDH1 depletion downregulates integrins and impairs chondrosarcoma growth. *Cancers (Basel)*. 2020;12:141.
73. Gallo E, Kelil A, Haughey M, et al. Inhibition of cancer cell adhesion, migration and proliferation by a bispecific antibody that targets two distinct epitopes on αv integrins. *J Mol Biol*. 2021;433:167090.
74. Bernstein AM, Twining SS, Warejcka DJ, Tall E, Masur SK. Urokinase receptor cleavage: a crucial step in fibroblast-to-myofibroblast differentiation. *Mol Biol Cell*. 2007;18:2716–2727.

Investigative Ophthalmology & Visual Science